Micromagnetic simulation of ferromagnetic part-spherical particles

Richard P. Boardman, Hans Fangohr, and Simon J Cox
Computational Engineering and Design Group
School of Engineering Sciences
University of Southampton
United Kingdom

Alexander V Goncharov, Alexander A Zhukov, and Peter A J de Groot
School of Physics and Astronomy
University of Southampton
United Kingdom
(Dated: December 3, 2003)

The paramagnetic size limit for current magnetic storage media, particularly in sputtered grain storage, is being approached rapidly. To further increase media storage density, patterned media can be used which only need a single grain to store one bit of data. Chemical self-assembly techniques offer cost-effective methods to create templates, from which periodic arrays of magnetic structures can be formed.

In contrast to systems of dots prepared by standard lithography, which have a cylindrical shape, dots prepared by chemical self-assembly template techniques are often spherical or part-spherical in shape. In this paper, we investigate the properties of such magnetic shapes using micromagnetic simulations. To represent accurately the geometry produced through chemical self-assembly methods, we attach a partial sphere (lower part) to a small ellipsoidal dome.

We compute the hysteresis loops for various dot sizes and compare them with experimental results. In those below a critical diameter (140nm in nickel), the hysteresis loop is square-like, resembling the uniform rotation of magnetisation once the critical field is exceeded. For larger sizes, the hysteresis loop reverses reversibly around zero applied field but shows minor loops, placed symmetrically at the onset of magnetisation reversal. These correspond to vortices penetrating and exiting the structure. In summary, we find that the coercive field of the droplets becomes zero above a critical diameter where the magnetisation reversal behaviour changes from single domain-like to vortex-like. Our results agree with experimental measurements performed on such structures.

INTRODUCTION

Current magnetic storage media types are approaching fundamental limits. The paramagnetic size limit for magnets causes those magnets which are below a particular size to become unstable at room temperature, capping their usefulness as long-term storage media. With traditional non-patterned media created by sputtering this problem is becoming more critical, as these grains are reduced whilst pursuing greater bit density. Since many grains are used to represent a single bit in non-patterned media, this severely limits the bit density that can be provided by this type of media.

One answer to this problem is to create patterned media which, by having a larger grain size, only need a single grain to store one bit of data; this then allows significant increase in the storage density of the media.

There are several different ways of creating patterned media. Photolithographic methods are limited down to half-micron sizes. Electron beam lithography is uneconomical when considered on a large scale.

Self-assembly methods appear to be a cost-effective way to create templates, from which an array of magnetic structures can be formed consisting of nanoclusters of atoms [1]. One particular method of chemical self-assembly involves the formation of templates through the evaporation of an aqueous suspension of polystyrene latex spheres [2], initiating the self-assembly. Using these spheres, it is possible to create magnetic structures from sizes of 50nm by filling the spaces between the close-packed spheres with some material through electrochemical deposition. By etching away the polystyrene spheres, a template is formed. This template can then be filled with magnetic material, and by varying the fill amount of the resulting spherical holes, connected or disconnected arrays of dots can be formed.

Previous work has shown that flat circular nanomagnets exhibit single-domain magnetisation reversal below a critical size and above this size will enter the vortex state around zero field [3–5]. In this work we investigate the behaviour of disjunct objects for a fill height smaller than half of the diameter of the spheres (see figure 1).

We simulate droplets resulting from the partial filling of templates with spherical voids. The measurements from the base to the top of the droplets are approximately $3/7d$, d being the diameter of the overall bounding sphere; the droplet follows the bounding sphere for $2/7d$ and the remaining $1/7d$ section is ellipsoidal (see figure 1).
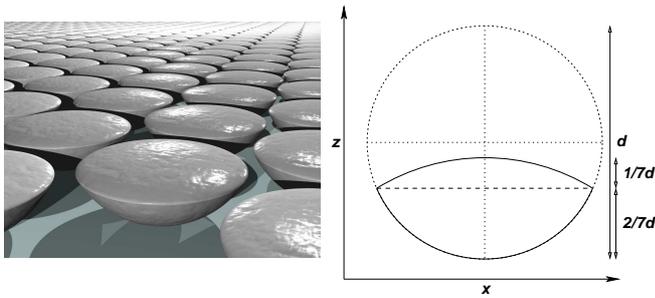
FIG. 1: (left) An artist's impression of an array of "droplets" representing the rounded ellipsoidal upper and (right) a cross-sectional diagram in which the solid line shows the droplet shape in the x-z plane

METHOD

We use the Object-Oriented MicroMagnetic Framework (OOMMF) software provided by the National Institute of Standards and Technology [6]. This software takes advantage of the Landau-Lifshitz Gilbert partial differential equation to solve problem environments [7]:

$$\frac{\mathrm{d}\mathbf{M}}{\mathrm{d}t} = -|\bar{\gamma}|\mathbf{M}\times\mathbf{H_{eff}} - \frac{|\bar{\gamma}|\alpha}{M_s}\mathbf{M}\times(\mathbf{M}\times\mathbf{H_{eff}}) \quad (1)$$

where $\mathbf{M}$ is the magnetisation (i.e. the magnetic moment per unit volume), $\mathbf{H}$ is the effective magnetic field, α is the Landau-Lifshitz phenomenological damping parameter and $\bar{\gamma}$ is the electron gyromagnetic ratio.

We simulate nickel, a slightly anisotropic material with an exchange coupling constant A of 9×10^{-12} J/m, a magnetisation M_s of 4.9×10^5 A/m. Comparative simulations show that the small anisotropy of nickel at room temperature does not affect the results presented in this work. We can calculate the exchange length for nickel from the equation $\sqrt{2A/\mu_0 M_s^2}$ [8]; in this instance it is about 8nm. This provides an indication of the necessary resolution of the numerical discretisation; if this granularity is unacceptably large, inaccuracies within the calculation arise associated with the angle between the magnetisation in two adjacent discrete cells [9]. In these simulations we use a discrete cell size of 5nm³; halving this and repeating the simulation leaves the results virtually unaffected indicating that it is not the finite difference discretisation which triggers the vortex.

Starting from an initially uniform magnetisation state in the x direction, we apply a high magnetic field capable of maintaining a homogeneous magnetisation and reduce this field until the magnetisation is reversed.

RESULTS

Figure 2 shows the hysteresis loop associated with a droplet of bounding sphere diameter d of 140nm; inset
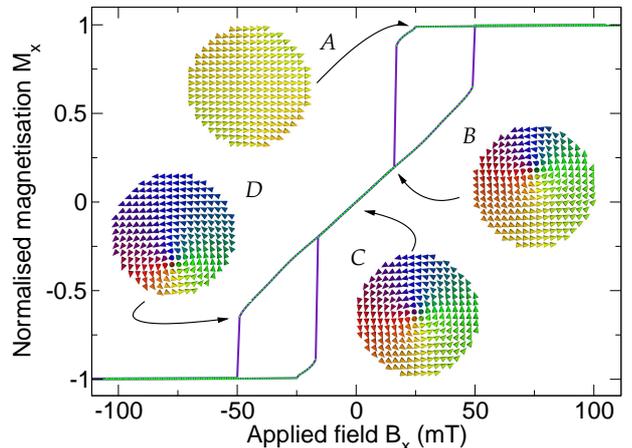
FIG. 2: Hysteresis loop with x-y cut-planes showing vortex propagation in a droplet with a bounding sphere diameter of $d = 140$nm.

with this loop are cross-sectional snapshots of the magnetisation during the reduction of the applied field. Initially, the magnetisation is homogeneous in the direction of the applied field (A). After reducing the field to approximately 25mT there is a slight drop in the net magnetisation; this is a precursor to vortex penetration. At around 15mT, the homogeneous magnetisation collapses into the vortex state (B). Reducing the applied field to zero results in the vortex shifting to the centre (C) and further reduction causes the vortex to move away from the centre (D). Finally, the applied field, now pointing in the negative x direction, forces the vortex out of the system, leaving the magnetisation pointing homogeneously in the x direction. The cross-sectional cut-planes show the states in the x-y plane whilst the field is being reduced.

At high fields (i.e. where $|\mathbf{B}| \geq 50$mT) the Zeeman energy dominates and the magnetisation is mainly aligned with this applied field. For small fields the vortex can move continuously in the system (insets B, C and D in figure 2). This allows the overall magnetic moment to follow the applied field, resulting in a reversibly linear $\mathbf{B} - \mathbf{M}$ characteristic around $|\mathbf{B}| = 0$. There is an energy barrier for a vortex to penetrate, form and disappear, which results in the two symmetrically placed hysteresis loops at 15mT $\leq |\mathbf{B}| \leq 50$mT. This hysteresis is similar to the behaviour in large ($d = 0.8\mu$m) cylindrical dots but very different to dots of the same size order [10, 11, for example] which show square-like and non-reversible hysteresis loops.

The associated hysteresis curves resulting from the simulations of droplets with bounding sphere sizes of 140nm, 350nm and 500nm are shown in figure 3. From these, we can see that although the overall behaviour in these three systems remains similar (i.e. vortex-like) there are slight changes in the shapes of the hysteresis
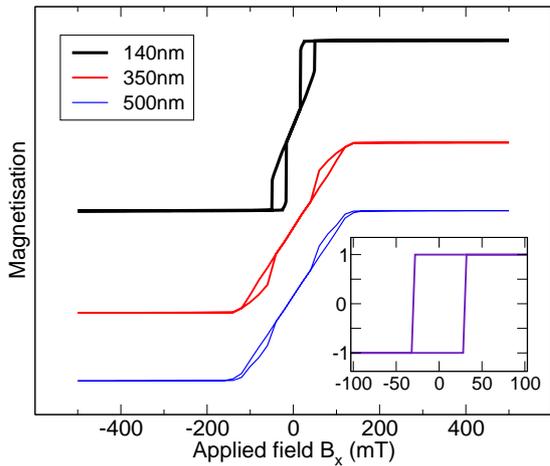
FIG. 3: Hysteresis loops for droplets of bounding sphere diameter 140nm, 350nm and 500nm; note that the loops are offset in the y direction for clarity. Inset is the hysteresis loop for a droplet of bounding sphere diameter 50nm

loops indicating that there is some change in the nucleation and disappearance methods of the vortex. The vortex penetration for these large systems shows behaviour which is related to that of spheres and will be described elsewhere [11].

We have studied size dependence by performing micromagnetic simulations on droplets of bounding sphere size between 20nm and 400nm. From this study we find that apart from a slight minimisation of the demagnetisation energy at the extremeties, the droplets behave as single domains at 130nm and below (see inset, figure 3), with a coercivity which increases as the bounding sphere diameter is reduced, and at 140nm and above the behaviour is vortex-like. Above this size, the coercive fields drop to zero as the droplets enter the vortex state. This is a significantly larger diameter than the value of 68nm for nickel spheres (calculated from $r_c = \sqrt{(9A/\mu_0 M_s^2)[\ln(2r_c/a) - 1]}$ [12]; this figure also agrees with our simulations of spheres to within a few mT [11]).

Figure 4 compares simulation results for a droplet of bounding sphere size 500nm with experimental results measured using a magneto-optical Kerr effect (MOKE) probe. A striking similarity can be seen between these results, particularly the vortex nucleation point (approximately 100mT) and the narrow openings in the hysteresis loop (around 50mT).

SUMMARY

We have simulated the magnetisation reversal in droplet nanodots, and we observe two different mechanisms for this reversal — the single-domain state and the vortex state.
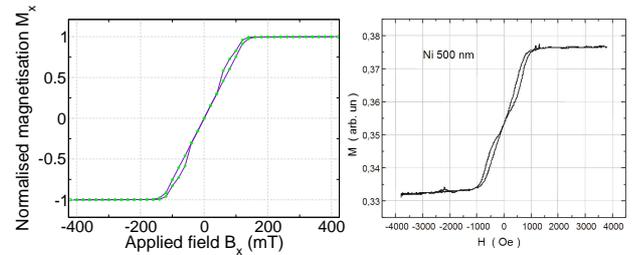
FIG. 4: Comparison between hysteresis loops from the simulation (left) and experimental measurement (right) of flat droplets with a bounding sphere diameter d of 500nm

If the overall size of the droplet system is increased then we notice a distinct transition from the single domain state to the vortex state, which we identify as being at a droplet bounding sphere radius of 140nm (physical droplet diameter in this instance is around 90% of the bounding sphere radius, approximately 126nm). This change occurs at a significantly smaller diameter than for thin circular nanodots.

The "soft" vortex behaviour (*i.e.* it will readily adjust its position to accommodate a change in applied field) observed in the large droplets is a useful characteristic in sensor applications; smaller droplets have the square hysteresis loops desirable for data storage.

ACKNOWLEDGEMENTS

[1] A. A. Zhukov, A. V. Goncharov, P. A. J. de Groot, P. N. Bartlett and M. A. Ghanem *Magnetic antidot arrays from self-assembly template methods* J. Appl. Phys. 93, 7322-7324 (2003)

[2] P. N. Bartlett, J. J. Baumberg, P. R. Birkin, M. A. Ghanem and M. C. Netti *Highly ordered macroporous gold and platinum films formed by electrochemical deposition through templates assembled from submicron diameter monodisperse polystyrene spheres* Chem. Mater., *14*, 2199-2208 (2002)

[3] R. P. Cowburn, D. K. Koltsov, A. O. Adeyeye, M. E. Welland and D. M. Tricker *Single-Domain Circular Nanomagnets* Phys. Rev. Lett. 83, 1042-1045 (1999)

[4] J. K. Ha, R. Hertel and J. Kirschner *Micromagnetic study of magnetic configurations in submicron permalloy disks* Phys. Rev. B 67, 224432 (2003)

[5] L. D. Buda, I. L. Prejbeanu, U. Ebels and K. Ounadjela *Micromagnetic simulations of magnetisation in circular cobalt dots* Comp. Mater. Sci 24, 181-185 (2002)

[6] M. J. Donahue and D. G. Porter *OOMMF User's Guide, Version 1.0* Interagency Report *NISTIR 6376*, National Institute of Standards and Technology, Gaithersburg, MD (1999)

[7] L. Landau and E. Lifshitz *On the theory of the dispersion of magnetic permeability in ferromagnetic bodies* Phys. Z. Sowjetunion 7, 153-169 (1935)

[8] H. N. Bertram and C. Seberino *Numerical simulations of hysteresis in longitudinal magnetic tape* J. Magn. Magn. Mater. 193, 388-394 (1999)

[9] M. J. Donahue and R. D. McMichael *Exchange energy representations in computational micromagnetics* Physica B, 233, 272-278 (1997)

[10] M. Schneider, H. Hoffmann and J. Zweck *Magnetisation reversal of thin submicron elliptical permalloy elements* J. Magn. Magn. Mater. 257, 1-10 (2002)

[11] R. P. Boardman and H. Fangohr *Magnetisation reversal in basic three-dimensional structures* In preparation

[12] R. C. O'Handley *Modern Magnetic Materials* Wiley Interscience (1999)